Influence of LME Cracks in Resistance Spot Welds of Zinc-coated Ultra-high Strength Steel Sheets on Joint Strength

Kyohei MAEDA*1 · Dr. Reiichi SUZUKI*1 · Masao HADANO*2

*1 Application Technology Center, Technical Development Group
*2 KOBELCO WELDING TechnoSolutions Co., LTD

Abstract

Liquid metal embrittlement (LME) cracking, seen in resistance spot welds of ultra-high strength steel, has become a subject of discussion in the automobile industry. However, only a few articles concerning the effect of this type of crack on joint properties have been reported. Therefore, in this study, LME cracks were classified into 3 types based on location and the influences of these cracks on static and fatigue strengths were investigated. Type A crack, occurring within an indentation of a spot weld, slightly affected the joint strength, while type B crack, generating on the indentation periphery or outside it, significantly lowered both tensile-shear and cross-tension strengths, which decreased by up to 35% and 44%, respectively. Type C crack, seen near the interface of the sheets, deteriorated fatigue strength as well.

Introduction

Since the 1990s, there has been a global demand for reducing greenhouse gases as a measure against global warming, with advocacy for achieving carbon neutrality by 2050. In the automotive industry, efforts are being made to decrease CO_2 emissions while driving by advancing the electrification and lightweighting of vehicle bodies[1), 2)]. The demand for collision safety is also increasing year by year. To achieve this, along with fuel efficiency, the application of ultra-high strength steel (referred to as "UHSS") sheets to vehicle bodies is on the rise. In the case of UHSS, alloying additives may be increased to balance strength and workability[3)]. Generally, it is known that welding properties deteriorate with an increase in alloying additives. For example, in resistance spot welding, mainly used in the production line of automobiles, expulsion and surface flash occur on the low current side, narrowing the condition range for proper welding[4), 5)]. In tensile tests, brittle fractures, such as interface failure and partial plug failure, occur, causing a decrease in joint strength[6)]. Furthermore, in some recently developed UHSSs, LME cracks caused by molten zinc have been reported to occur during the welding of Zn-coated steel sheets[7)-9)]. As shown in **Fig. 1**, LME cracks occur when three factors overlap: high crack susceptibility, molten zinc, and tensile stress.

In other words, if any one of these factors can be eliminated, the cracking can be prevented. Previous studies have demonstrated through numerical analysis that significant tensile stress occurs in the welded area immediately after electrode release[10)]. Suggestions have been proposed to mitigate LME cracking through process enhancements, specifically targeting stress alleviation and minimizing the volume of molten zinc during electrode release[10)-15)]. On the other hand, welding conditions are often restricted by production cycle time and part shapes, making it not always possible to apply these crack prevention methods. Therefore, to effectively utilize UHSS, it is believed that optimization of welding conditions alone is not sufficient, and structure design allowing the presence of LME cracks is also necessary. Generally, in the design of automobiles, the required strength in the welding area is calculated on the basis of the loads applied during both driving and collision. For spot welding, JIS Z 3140 specifies required values for tensile-shear strength (TSS) and cross-tension strength (CTS) for each category of sheet thickness and strength, and these may be used as indicators during design. Even if LME cracks occur, there is a possibility of expanding the application range of ultra-high-tensile steel by adopting a structural design approach that allows for cracks as long as the standard strength is achieved. A similar approach is adopted in JIS Z

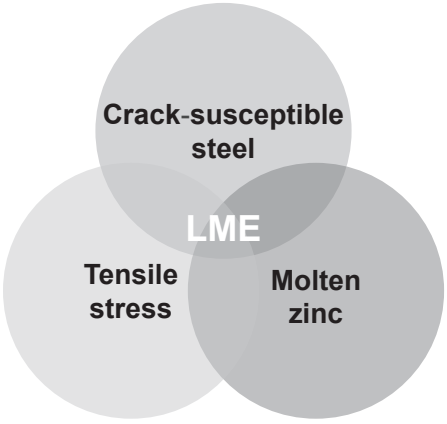

Fig.1 Factors of LME cracking

3104, where, among the four categories of scratches (defects), the first and fourth categories need not be counted if they are below certain dimensions. However, data regarding the effects of LME cracks on joint strength is limited, and as of now, there are no established standards for LME cracks. Against this backdrop, this study aims to classify LME cracks in accordance with their occurrence locations and elucidate the effects of various cracks on static strength and fatigue strength.

1. Experimental method

1.1 Classification of LME cracks

LME cracks are broadly categorized into outer cracks occurring on the surfaces of joints and inner cracks occurring internally[16]. As shown in **Fig. 2**, this study further classifies the outer cracks into type A cracks, which occur within an indentation, and type B cracks, which occur at the periphery of an indentation. Inner cracks occurring in the heat-affected zone (HAZ) are classified as type C cracks.

1.2 Investigation of the effects of LME cracks on static strength and fatigue strength

The test material used was a 980MPa-grade GA steel sheet with a thickness of 1.4 mm. For the static tensile test, the test pieces were prepared in accordance with JIS Z 3136 and Z 3137, and for the fatigue test, the test pieces followed Z 3138, with the size as shown in **Fig. 3**. The steel sheets were immersed in hydrochloric acid, creating samples with a remaining plating layer on only one side near the welded area (hereinafter referred to as "plated material") and samples with all plating layers removed on both sides (hereinafter referred to as "bare material").

A servo-pressure-type DC inverter welding machine was used for welding. The electrodes were DR-type electrodes made of chrome copper, with a tip diameter of 6 mm and a tip curvature radius of 40 mm. The welding conditions are shown in **Fig. 4**, and the schematic diagram of the joint preparation method is illustrated in **Fig. 5**.

The plated material was used to control the initiation positions of cracks; i.e., for outer cracks, the plated surfaces of the upper and lower sheets were positioned facing the electrode, and for inner cracks, they were positioned facing the side of the mating material. For the latter, aiming at promoting crack formation, a strike angle of 7° was set, and a 2 mm gap was introduced between the sheets. For comparison, joints with no cracks but having a nugget with a diameter equivalent to the joint with outer and inner cracks were produced using the bare material (hereinafter referred to as "defect-free jointing"). The type B cracks have initiated from the periphery of the indentation to the outside, and it

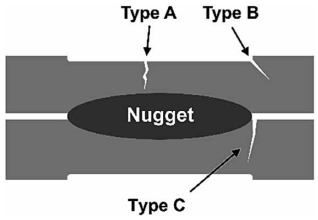

Fig.2 Classification of LME cracks

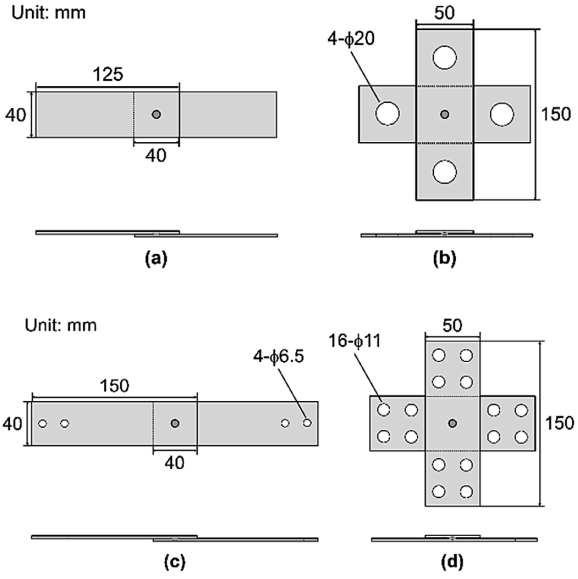

Fig.3 Dimensions of tensile specimens
(a) static tensile-shear, (b) static cross-tension tests
(c) tensile-shear fatigue, (d) cross-tension fatigue tests

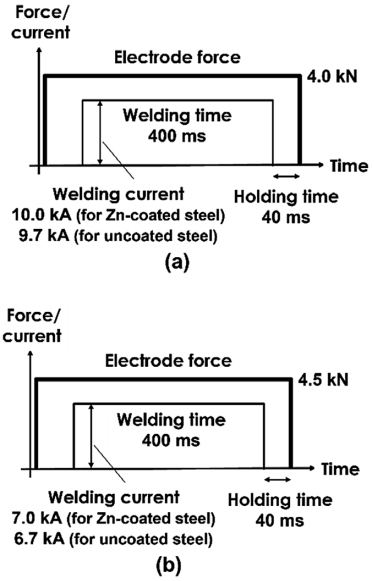

Fig.4 Welding conditions for producing welds with LME
(a) outer, (b) inner cracks

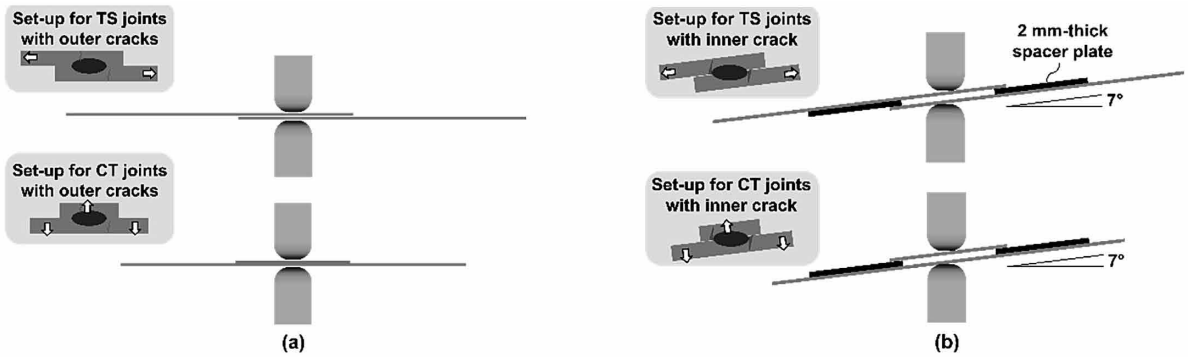

Fig.5 Schematic illustration of set-up for producing welds with LME (a) outer, (b) inner cracks

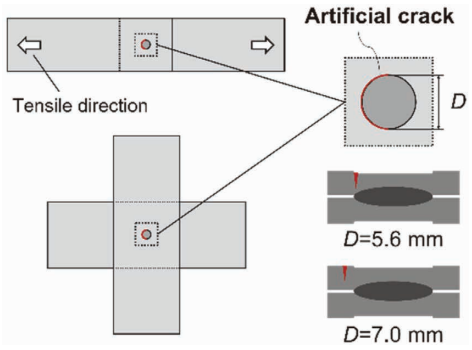

Fig.6 Schematic illustration of creating artificial crack in welds

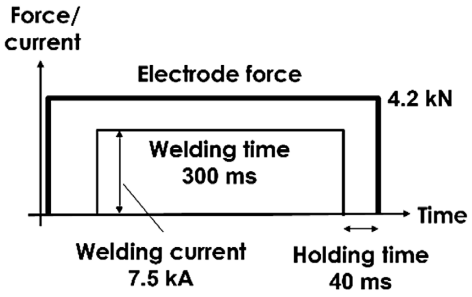

Fig.7 Welding conditions for producing welds without crack

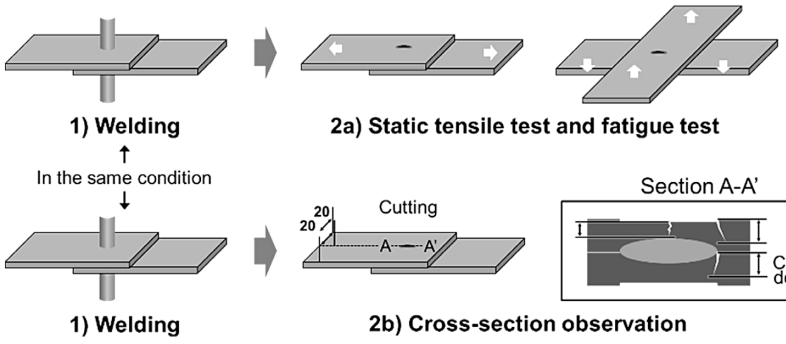

Crack	Static tensile test	Fatigue test
Type A	✓	✓
Type A+B	✓	-
Artificial type B	✓	✓
Type C	✓	✓

Fig.8 Process flow of testing and evaluation

is assumed that the degree of adverse effects varies depending on the location of initiation. Controlling the subtle initiation positions of cracks through welding is challenging. Hence, the cracks were simulated using a femtosecond laser. As shown in **Fig. 6**, joint strength at various initiation positions was investigated by forming a semi-circular groove with a width of millimeter-order (hereinafter referred to as an "artificial defect") on a defect-free joint. After welding the bare material under the conditions shown in **Fig. 7**, artificial defects were introduced to the inner and outer peripheries and outside of the indentation on the side of the upper sheet. The diameter of the artificial defect was 5.6 mm for the former and 7.0 mm for the latter. The flow of evaluation tests for the prepared joints is shown in **Fig. 8**. Two types of static tensile tests (tensile-shear test and cross-tensile test) and two types of fatigue tests (tensile-shear fatigue test and cross-tension fatigue test) were conducted. The number of samples (denoted by a numerical value following n) for the static tensile test was n3 to n5, and the tensile speed was set at 10 mm/min. Fatigue tests were conducted for n2 at each load, with a stress ratio of 0.1, frequency of 5 to 20 Hz, and a maximum repetition number of 2×10^6. It should be noted that, for joints where outer cracks were induced experimentally, some included only type A cracks, and others included both type A and B cracks. Therefore, visual observation with a microscope was conducted, and for the former, both static tensile and fatigue tests were performed, while

for the latter, only static tensile tests were conducted. Additionally, cross-sectional observations were carried out for another set of n3 samples apart from the tensile test. Observations of the welded area were conducted by cutting the center of the nugget in the tensile-shear test piece along the longitudinal section, followed by corrosion in a picric acid-saturated solution, and examination using an optical microscope. The depth of the cracks was measured following the procedure shown in Fig. 8.

2. Experimental results and discussions

2.1 Effect of outer cracks on static strength and fatigue strength

The appearances and cross-sections of the joints are shown in **Fig. 9**. A joint with only type A cracks (b) has been checked as well as a joint with both type A and B cracks (c) (hereinafter referred to as "joint with type-A cracks" and "joint with type A+B cracks," respectively). The depths of the type A and B cracks are 0.07 to 2.13 mm and 0.07 to 0.91 mm, respectively, and the type A cracks have been observed to penetrate both surfaces of the indentation.

The results of the static tensile test are shown in **Fig.10**. In the lower part of the graph, the types of cracks are also described. In comparison with the defect-free joint, the joints with type A cracks have been found to have equivalent joint strength, confirming that the type A cracks have little effect on static strength. On the other hand, the joints with type A+B-cracks have cases where TSS and CTS are lower than the defect-free joint. When comparing the joint strength of the lowest strength combinations, the joints with type A+B cracks show an approximately 35% reduction in both TSS and CTS compared with the defect-free joint. **Fig.11** shows the appearances of the joints with type A+B cracks before and after the tensile tests. Also included in this figure are the crack initiation positions, and the schematic diagrams of fracture positions during the tensile test. For the tensile-shear test joint, the crack initiation positions have been classified into the transverse area and longitudinal area, as shown in this figure. In both joints, fractures have occurred along the type B cracks. For joints with a small crack initiation zone in the transverse area, TSS is almost equivalent to that of the defect-free joint. In contrast, joints with a wide-ranging presence of cracks exhibit a significant decrease in TSS. In the cross-tension testing, stress is uniformly applied at the periphery of the nugget, resulting in a decrease in strength regardless of the location of crack initiation. In contrast, in shear-tension testing, stress concentration primarily occurs in the transverse area. Therefore, cracks that occur in the longitudinal area are believed to have minimal impact on the overall strength. The results of fatigue test for the

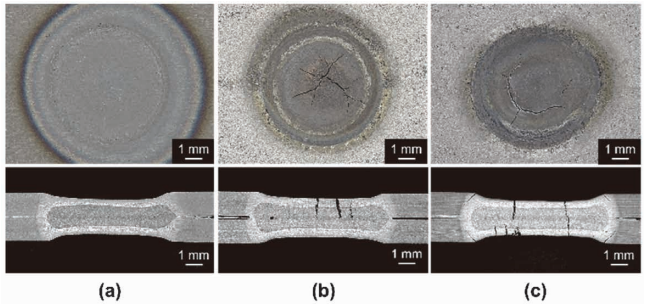

Fig.9 Surface and cross-section images of welds
(a) without LME crack, (b) with type A crack, (c) with type A+B cracks

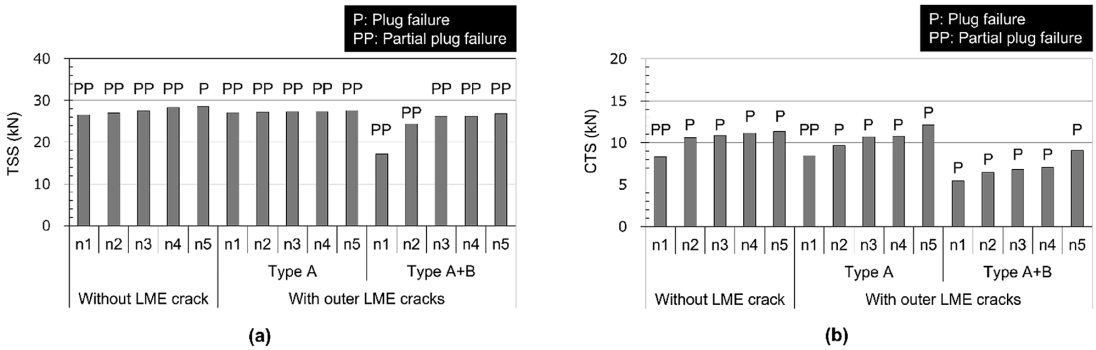

Fig.10 Results of static (a) TS, (b) CT tests

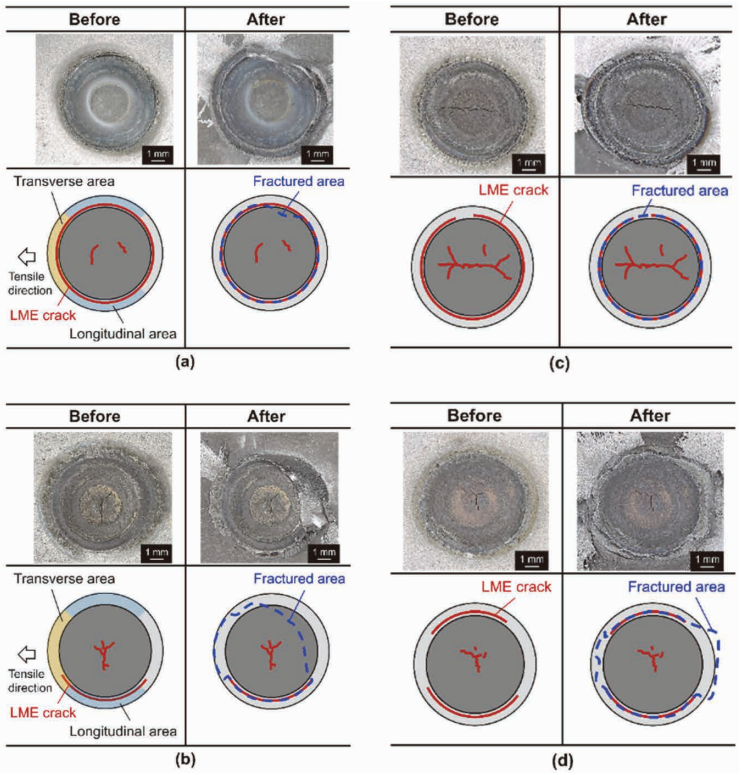

Fig.11 Surface view of specimens with type A+B cracks before and after static tensile tests (TS test: (a)n1, (b)n3, CT test: (c)n1, (d)n4)

joint with type A cracks and the defect-free joint are shown in **Fig.12**. No significant difference has been observed in the L-N diagram due to the presence or absence of type A cracks, indicating that type A cracks have little effect on fatigue properties.

2.2 Effect of occurrence position for Type B cracks on static strength and fatigue strength (Results of study utilizing artificial defects)

The appearance and cross-sectional images of the joint are shown in **Fig.13**. The depths of artificial defects at the inner and outer peripheries of the indentation and the outside of the indentation are 0.55 to 0.63 mm and 0.54 to 0.61 mm, respectively. The results of the static tensile test are presented in **Fig.14**. For joints with artificial defects at the inner and outer peripheries of the indentation, TSS is equivalent, while CTS is lower in comparison with the defect-free joint. On the other hand, for joints with artificial defects on the outside of the indentation, a slight decrease in TSS, in addition to CTS, is observed. When the lowest CTS values are compared, the former joint shows approximately a 35% reduction in strength compared with the defect-free joint, and the latter joint shows approximately a 44% reduction. This suggests that the further away from the indentation, the greater the negative impact on cracks. In comparison with the tests

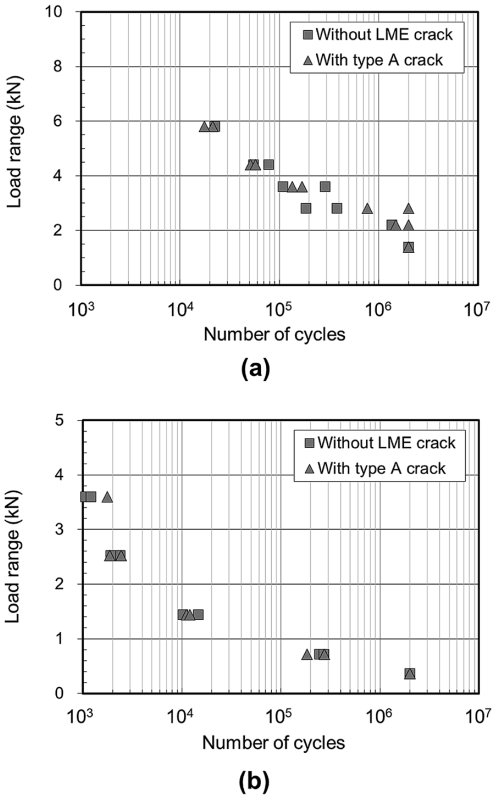

Fig.12 Results of (a) TS, (b) CT fatigue tests

using the previously mentioned joint with type A+B cracks, no significant decrease in TSS has been observed in joints with introduced artificial defects.

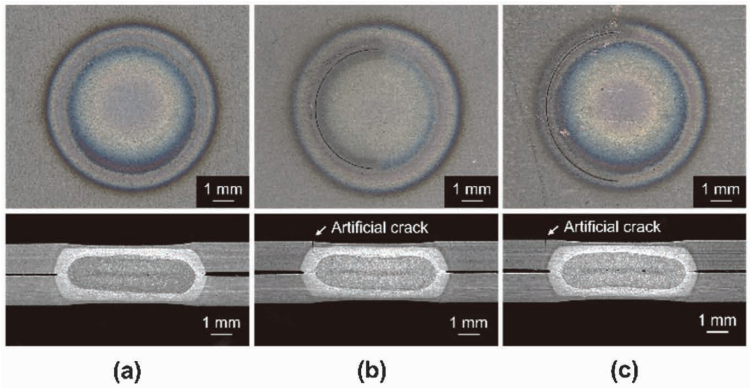

Fig.13 Surface and cross-section images of welds
(a) without crack, with artificial crack (b) on indentation periphery, (c) outside indentation

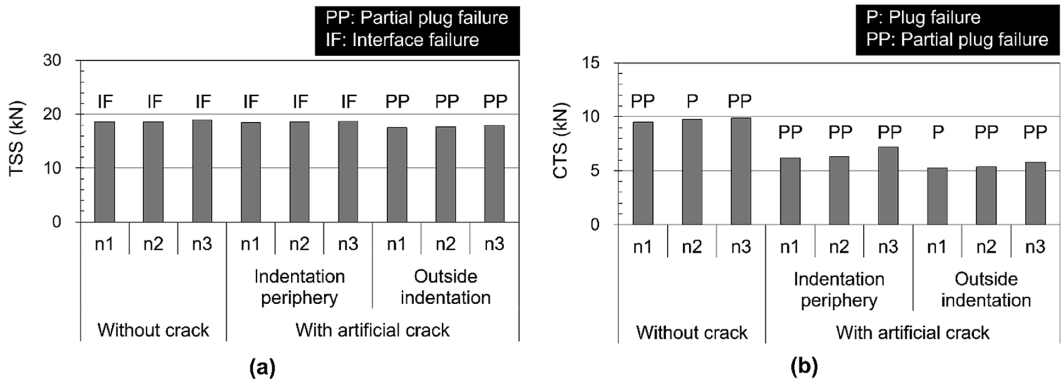

Fig.14 Results of static (a) TS, (b) CT tests

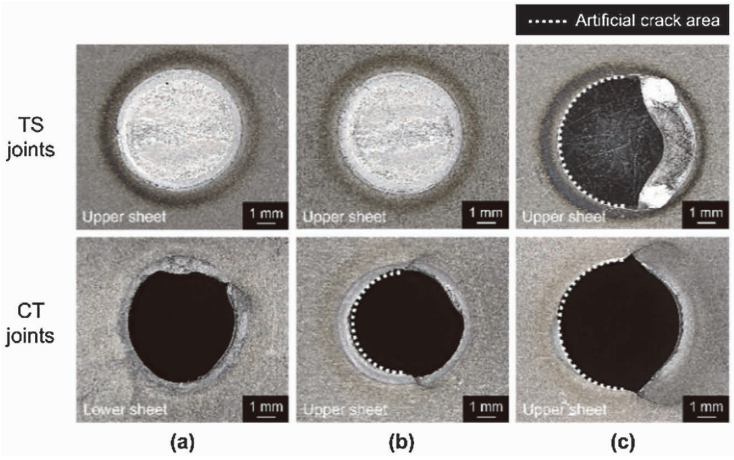

Fig.15 Surface view of fractured TS and CT specimens
(a) without crack, with artificial crack (b) on indentation periphery, (c) outside indentation

This is presumed to be due to the difference in size between actual cracks and artificial defects. Due to constraints in the laser processing machine used in this experiment, the depth of artificial defects has been aimed at 0.6 mm, which is smaller than the actual depth of the type B cracks. In a previous study based on numerical analysis, Ma et al. have demonstrated that the reduction in tensile-shear strength is enhanced with the increasing size of the type B cracks[17]. Appearance images after tensile-shear and cross-tensile tests are shown in **Fig.15**. In joints where a decrease in strength has been observed, fractures have occurred along the artificial defects. The results of the fatigue test are presented in **Fig.16**. No significant differences are observed in the L-N diagram due to the presence or absence of artificial defects. In other words, in the range of depths equivalent to the artificial defects studied in this experiment, there is a high probability that the fatigue properties would not significantly decrease

due to type B cracks.

2.3 Effect of inner cracks on static strength and fatigue strength

Fig.17 shows the cross-sectional images of joints. Type C cracks have been observed at the corona bond edges of the upper and lower sheets (hereinafter referred to as a "joint with type C cracks"). The depth of the cracks ranges from 0.25 to 0.79 mm. The results of the static tensile test are presented in **Fig.18**. Within the range studied in this experiment, there is little decrease in joint strength due to inner cracks. Both the joint with type C cracks and the defect-free joint exhibit interface fractures in the tensile-shear test and plug fractures or partial plug fractures in the cross-tensile test. Although no changes are observed in joint strength or fracture morphology due to the presence of inner cracks in this experiment, a study using 1.2 GPa-grade steel sheets confirmed a reduction in TSS due to the type C cracks[18]. The reasons for the varying effect of cracks due to differences in steel sheet strength are not clearly understood. However, it is speculated that the distribution of stress during the tensile-shear test may change depending on the hardness distribution in the nugget-HAZ-base metal interfaces and the depth of the cracks. In the case of 1.2 GPa-grade steel sheets, it is presumed

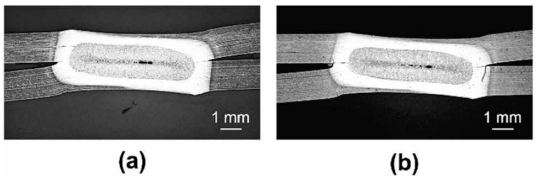

Fig.17 Cross-section images of welds
(a) without LME crack, (b) with type C crack

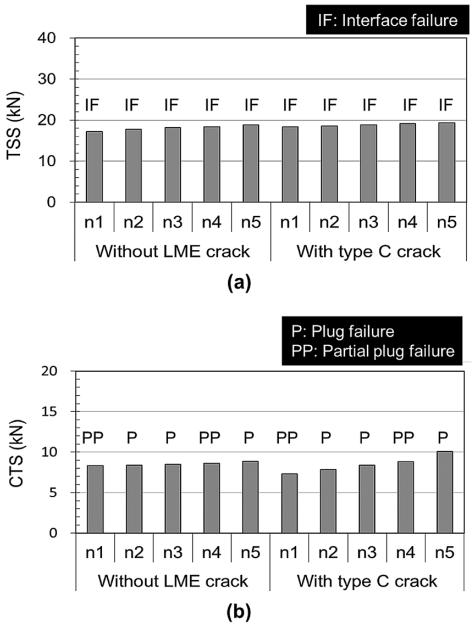

Fig.18 Results of static (a) TS, (b) CT tests

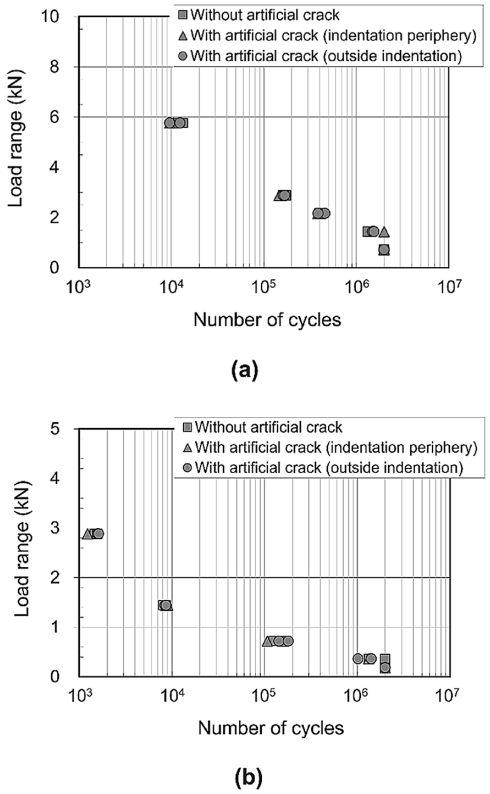

Fig.16 Results of (a) TS, (b) CT fatigue tests

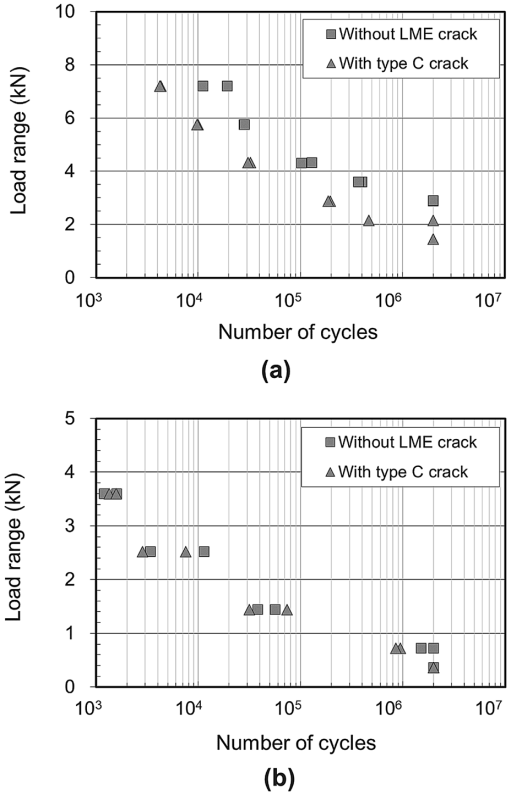

Fig.19 Results of (a) TS, (b) CT fatigue tests

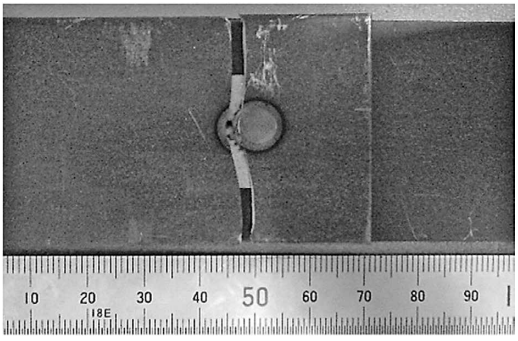

Fig.20 Surface view of fractured TS fatigue specimen with type C crack

that the stress concentration on the type C cracks is more pronounced. The results of the fatigue test are shown in **Fig.19**. No significant differences are observed in the L-N diagrams for cross-tension fatigue tests between the joint with type C cracks and the defect-free joint. On the other hand, in the tensile-shear fatigue test, early fractures occur in the joint with type C cracks under all load conditions, indicating that type C cracks lead to a reduction in fatigue properties. As shown in **Fig.20**, cracks have propagated from around the nugget towards the base metal in the joint with Type C cracks, suggesting that type C cracks may have served as the initiation point for the cracks. Initial cracks in tensile-shear fatigue tests have been reported to occur near the corona bond edges[19]. As type C cracks occur in almost the same position as these cracks, they are considered a potential factor contributing to the reduction in fatigue properties.

Conclusions

LME cracks have been classified into types A to C, and their respective effects on joint strength have been experimentally investigated. The summarized results are shown in **Fig.21**. Regarding type A cracks, even those penetrating through both the surfaces have little effect on joint strength. In contrast, it has become evident that type B and C cracks could potentially reduce joint strength. It should be noted that, in this study, tensile tests and cross-sectional observations have been conducted separately; hence, a thorough discussion on the relationship between joint strength and crack depth has not been provided. In a previous study[18], the authors have attempted to quantify the effect of crack depth on joint strength by non-destructively observing LME cracks in tensile test samples using X-ray CT scans. As mentioned earlier, the adverse effects of LME cracks vary with steel types and sheet compositions. Performing tests for a vast range of steel types and sheet compositions similar to this study is impractical. Therefore, the use of numerical analysis is essential. The authors have already begun numerical analysis and have constructed a model that can predict the effects of cracks at the test piece level[17]. Furthermore, the investigation into the effect of LME cracks at the level of actual vehicle components is ongoing. Dynamic three-point bending tests have been conducted on simulated center pillar samples with artificially induced outer and inner cracks. The results have revealed that, under assumed IIHS side impact distribution conditions, the presence of LME cracks did not lead to the fracture of resistance spot welded parts. The effects on component performance, such as maximum load and absorbed energy, have been found to be extremely small [20]. Vehicle lightweighting is a persistent need, and the application of ultra-high tensile steel is predicted to further expand in the future. While multiple spot welding processes for preventing LME cracks have

Crack type		Crack depth (mm)	Static strength		Fatigue strength	
			TS	CT	TS	CT
A	Weld crack	0.07～2.13	Influenced slightly	Influenced slightly	Influenced slightly	Influenced slightly
B	Weld crack	0.07～0.91	**Weakened**	**Weakened**	-	-
	Artificial crack	Approximately 0.60	Influenced slightly[1)]	**Weakened**	Influenced slightly	Influenced slightly
C	Weld crack	0.25～0.79	Influenced slightly[2)]	Influenced slightly	**Weakened**	Influenced slightly

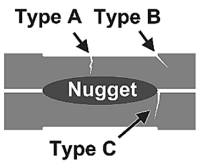

1) TSS might be weakened with a greater artificial crack.
2) The result of the experiment using 1 GPa steel.
Type C crack weakened TSS of spot welds of 1.2 GPa steel.

Fig.21 Summary of experiments

been developed and proposed, establishing quality assurance methods for LME cracks is also deemed necessary. It is hoped that the approaches and insights introduced in this paper can contribute to these efforts.

References

1) Y. Miyazaki et al. Journal of Japan Laser Processing Society. 2019, Vol.26, No.1, pp.13-23.
2) D. Tarui. Journal of the Japan Society of Precision Engineering. 2018, Vol.84, No.5, pp.404-407.
3) H. Matsuda. Journal of the Japan Welding Society. 2020, Vol.89, No.6, pp.420-424.
4) K. Yamazaki et al. Quarterly Journal of the Japan Welding Society. 1999, Vol.17, No.4, pp.553-560.
5) H. Oikawa et al. Nippon Steel Technical Report. 2006, No.385, pp.36-41.
6) R. Ikeda. Journal of the Japan Welding Society. 2015, Vol.84, No.6, pp.11-16.
7) A. G. Kalashami et al. Journal of Manufacturing Processes. 2020, Vol.57, pp.370-379.
8) R. Sierlinger et al. White Paper; voestalpine Stahl GmbH. 2016, pp.1-16.
9) G. Jung et al. Metals and Materials International. 2016, Vol.22, No.2, pp.187-195.
10) K. Takashima. Welding Journal. 2021, Vol.90, No.7, pp.24-28.
11) C. Bohne et al. Science and Technology of Welding and Joining. 2020, Vol.25, No.7, pp.617-624.
12) C. Bohne et al. Science and Technology of Welding and Joining. 2020, Vol.25, No.4, pp.303-310.
13) E. Wintjes et al. Journal of Manufacturing Science and Engineering. 2019, Vol.141, No.10, Article 101001, 9p.
14) K. Maeda et al. Prevention of LME Cracks in Resistance Spot Welding by Optimization of Pressure and Welding Current. Preprints of the National Meeting of JWS. The Japan Welding Society, 2020, pp.130-131.
15) Y. Shimoda et al. Development of Prevention Method for LME Cracks in Resistance Spot Welding of Zinc-Coated Ultra-High Tensile Steel Sheets - Development of Mechanical Upset Control Shank. Preprints of the National Meeting of JWS. The Japan Welding Society, 2020, pp.132-133.
16) O. Siar et al. Metals. 2020, Vol.10, No.9, Article 1166.
17) Y. Ma et al. Materials & Design. 2021, Vol.210, Article 110075, p.21.
18) K. Maeda et al. Quarterly Journal of the Japan Welding Society. 2022, Vol.40, No.3, pp.123-133.
19) Y. Uematsu et al. Quarterly Journal of the Japan Welding Society. 2019, Vol.37, No.4, pp.152-161.
20) N. Mizutani et al. Effect of Resistance Spot Welding LME Cracks in Hat Section Parts on Part Performance. JSAE Autum Convention Proceedings. The Japan Welding Society, Society of Automotive Engineers of Japan. 2021, Article 20216153.